Design of Wideband Dual-Band Substrate Integrated Waveguide Slot Antenna

Wanpeng CHEN, Jiexin YU, Ziwen YANG, Xiaolin YANG

University of Electronic Science and Technology of China, Chengdu, Sichuan 611731, China

yxlin@uestc.edu.cn

Submitted May 13, 2024 / Accepted August 27, 2024 / Online first October 31, 2024

Abstract. *A dual-band Half Mode Substrate Integrated Waveguide (HMSIW) slot antenna operating at 3.5 GHz and 4.9 GHz is proposed. The two operational bands of the proposed antenna are achieved by combining two HMSIW slot antennas. The –10 dB impedance bandwidth and realized gain of the antenna at 3.5 GHz and 4.9 GHz are 3.47–3.68 GHz with a gain of 3.9 dBi and 4.62–5.16 GHz with a gain of 5.5 dBi, respectively. Compared with the traditional SIW dual-band antenna, the bandwidth of the antenna has been significantly improved. The proposed antenna has a simple structure and exhibits excellent radiation performance in both operating frequency bands, making it suitable for 5G mobile communication systems.*

Keywords

Half Mode Substrate Integrated Waveguide (HMSIW) antenna, antenna miniaturization, cavity-backed slot antenna

1. Introduction

Substrate Integrated Waveguide (SIW) has the advantages of low loss, small size and easy integration with microstrip circuits, which is suitable for microwave and millimeter-wave circuits. Since Substrate Integrated Waveguide was proposed, this technology has been widely applied in various microwave devices, such as filters [1–4], power dividers [5–7] and antennas [8–12].

A SIW quasi-elliptic filters with mixed electric and magnetic coupling are proposed in [1]. Due to high Q of evanescent-mode SIW cavity resonators, narrowband filters can be obtained [2]. For reducing the loss, an empty waveguide integrated into a dielectric substrate is proposed to realize the high-performance microwave filter [3]. SIWs also are used to integrate filter and amplifier to form the compact filter-amplifier device [4]. In [5], an eight-way-band SIW radial cavity power divider with low insertion loss is reported. To miniaturize the power dividers, one-eighth mode SIW resonator is used in [6]. The SIW based on low temperature co-fired ceramic technique is also used to design the power dividers [7].

Due to narrow bandwidth is an inherent disadvantage of cavity-backed slot antenna, expanding the bandwidth is a hot research direction for SIW slot antenna. A broadband SIW cavity-backed slot antenna is proposed in [8]. The frequency corresponding to the TE_{110} mode of the rectangular SIW cavity is 9.2 GHz. With the introduction of the butterfly slot, the frequency corresponding to the TE_{120} mode was shifted from 14.7 GHz to 10.52 GHz. The two hybrid modes expand the bandwidth to 9.4%. Changing the shape of the slot to excite multiple modes of SIW cavity can also expand the bandwidth of the SIW antenna [9]. In [10], the slot was changed to a trapezoidal shape to improve the bandwidth, and the influence of the trapezoidal slot was analyzed. Adding shorted via is another common way to expand the bandwidth [11].

Compared with the SIW cavity, the size of the HMSIW cavity is reduced in half. The size of the antenna using HMSIW is greatly reduced while the radiation performance is not changed, which is suitable for miniaturized microwave and millimeter-wave systems. A wideband SIW slot antenna using HMSIW technology is proposed in [12]. The antenna utilizes three-mode coupling to extend the bandwidth, and the bandwidth of the antenna is 11.7%. A Ka-band leaky-wave antenna array based on HMSIW structure is proposed in [13]. A miniaturized self-triplexing antenna based on shielded half-mode substrate integrated waveguide was designed in the article [14]. An improved inverted U-shaped groove was created on the top plane of the cavity to form three different radiation patches, and the antenna has a compact structure.

For some wireless communication systems, it is necessary for antennas to operate at several different frequencies simultaneously. SIW antennas can adjust various resonance modes by adding through holes and slots to achieve a dual-band. A dual-frequency SIW slot antenna using a new dumbbell-shaped slot is proposed [15]. This antenna operates at 9.5 GHz and 13.85 GHz, with a bandwidth of approximately 1.5%, and gains of 4.8 dBi and 3.7 dBi at the two frequencies, respectively. In [16], the SIW slot antennas were used to radiate in the X-band, and radiates in the C-band through the patch elements of the microstrip antenna. In [17], a miniaturized cylindrical open SIW cavity is designed, allowing it to operate in two frequency bands. In [18], dual-band radiation by adding through holes is achieved. However, the

DOI: 10.13164/re.2024.0636

bandwidth of dual-band antenna with a single SIW cavity is relatively narrow.

In this work, a dual-band HMSIW slot antenna with bandwidth enhanced operating at 3.5 GHz and 4.9 GHz is proposed. Two HMSIW slot antennas are integrated to achieve dual-band antenna. Although two HMSIW slot antennas are used to realize dual frequency, the size of the proposed HMSIW antenna is almost the same as single cavity SIW antenna, while the bandwidth is wider than that of single cavity SIW antenna.

2. Antenna Design

According to the design of SIW, when the distance between metal vias is much smaller than the wavelength of the waveguide, the SIW cavity can be equivalent to a rectangular waveguide. The cut frequency of the SIW can be expressed as [19]:

$$f_{mn}=\frac{c}{2\sqrt{\varepsilon_r\mu_r}}\cdot\sqrt{\left(\frac{m}{W_{\text{eff}}}\right)^2+\left(\frac{n}{L_{\text{eff}}}\right)^2} \tag{1}$$

where

$$W_{\text{eff}}=W-1.08\frac{d^2}{p}+0.1\frac{d^2}{W},$$

$$L_{\text{eff}}=L-1.08\frac{d^2}{p}+0.1\frac{d^2}{L}$$

are the effective width and length of the SIW cavity, respectively. The others parameters are dielectric constant ε_r, magnetic permeability μ_r, standing waves numbers m and n, actual cavity width W, actual cavity length L, via diameter d, distance between vias p. The field modes of the HMSIW are same as those of SIW [20].

The data comes from the HFSS 15.0 simulator. Figure 1 shows the configuration of the proposed antenna. The substrate is Rogers RT 5880 with a thickness of 1.575 mm ($\varepsilon_r = 2.2$, $\tan\delta = 0.0009$). The antenna includes two HMSIW cavities with different sizes corresponding to two frequency bands of 3.5 GHz (right cavity) and 4.9 GHz (left cavity), respectively. A shorted via is placed in the middle of each cavity to perturb the field of the cavity, which is used to expand the bandwidth of the antenna. Two trapezoidal slots are located on the top layer. The feeding structure is located on the bottom layer, where a transition of 50 Ω microstrip line to 100 Ω coplanar waveguide is adopted to feed two HMSIW cavities, respectively. Table 1 shows the parameters of the proposed antennas.

Figure 2 shows the design process of the proposed dual-band SIW antenna. According to (1), the cavity size of Antenna I was set as 21.5 mm × 52.4 mm to meet the resonant frequency of 3.5 GHz, while the cavity size of Antenna II was set as 21.5 mm × 72.0 mm to meet the resonant frequency of 5.0 GHz. Combining Antenna I and Antenna II forms the proposed antenna, that is, the dual-band antenna is obtained.

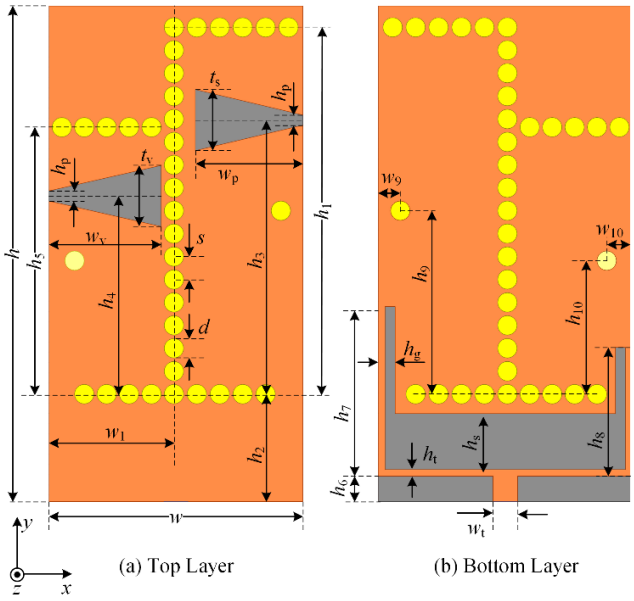

Fig. 1. Configuration of the proposed dual-band SIW slot antenna. (a) Top layer and (b) Bottom layer.

Parameter	Values (mm)	Parameter	Values (mm)
w	49.8	h_5	52.4
h	97.3	h_6	5
d	3.8	h_7	33.3
s	4.4	h_8	25.3
t_s	12	h_9	36
t_v	10	h_{10}	26.2
h_p	2	w_1	24.5
h_1	72	w_v	22
h_2	22	w_p	21.1
h_3	52.8	w_9	4.3
w_t	4.8	w_{10}	5.2
h_4	37.9	h_g	2
h_t	1.3		

Tab. 1. Parameters of the proposed antenna.

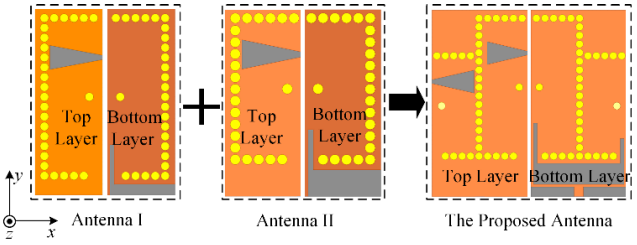

Fig. 2. Illustration of antenna design process.

In order to widen the bandwidth, a shorted via is introduced to each of Antenna I and Antenna II. Figure 3 and Figure 4 show the simulated reflection coefficients of Antenna I and Antenna II with and without a shorted via. It can be observed that the introduction of the shorted via has significantly improved the impedance bandwidth and reflection coefficients of the antennas.

The key parameters influence on antenna response are studied. Figure 5 shows reflection coefficient of the proposed antenna with different location of the trapezoid slots. It can be seen that the location of the trapezoid slots has significant effect on resonant frequency and bandwidth. The reflection coefficients of the proposed antenna with different

size of the trapezoid slots are given in Fig. 6, which indicates that size of the trapezoid slots has slight effect on S_{11}. Figure 7 shows the reflection coefficient of the proposed antenna with different location of the shorted via. It can be seen that the location of the shorted via affects the bandwidth. Moreover, the parameters study also shows that the lower frequency band of 3.5 GHz and the high frequency band of 4.9 GHz can be controlled independently.

Figures 8 and 9 depict the electric field distributions of Antenna I and Antenna II with and without the shorted via. For Antenna I, without the shorted via, the resonant frequency of the TE_{110} mode is 2.2 GHz, and the resonant frequency of the TE_{120} mode is 3.7 GHz. By introducing the shorted via, the electric field of the TE_{110} mode is severely disturbed, while the electric field of the TE_{120} mode is hardly affected. This shift means that the resonant frequency of the TE_{110} mode is shifted from 2.2 GHz to around 3.45 GHz, resulting in multi-mode resonance, which extends the bandwidth of the antenna. Similar situations occurred in Antenna II.

Figure 10 shows the simulated realized gains of Antenna I, Antenna II, and the proposed antenna. It can be seen that combining Antenna I and Antenna II in this way has slight effect on the gain. These results also indicate that feed network also has little impact on the proposed antenna.

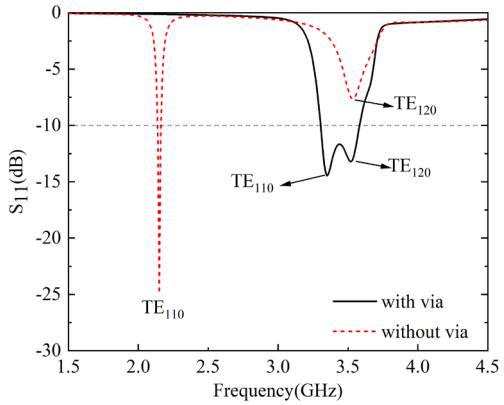

Fig. 3. Simulated reflection coefficient of Antenna I with and without via.

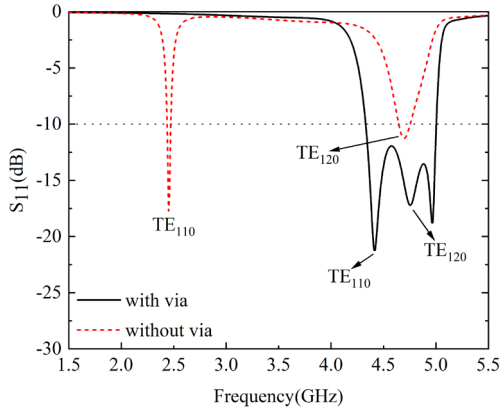

Fig. 4. Simulated reflection coefficient of Antenna II with and without via.

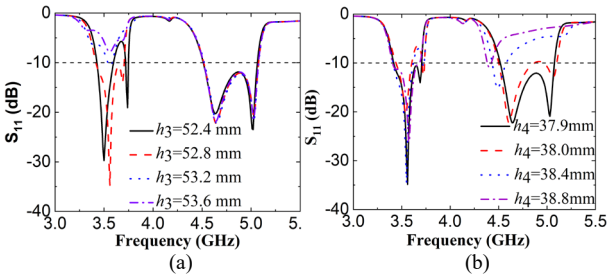

Fig. 5. Reflection coefficient of the proposed antenna with different location of the slots. (a) S_{11} with different h_3, and (b) S_{11} with different h_4.

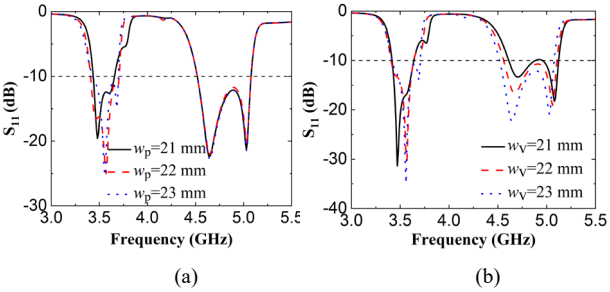

Fig. 6. Reflection coefficient of the proposed antenna with different size of the slots. (a) S_{11} with different w_p, and (b) S_{11} with different w_v.

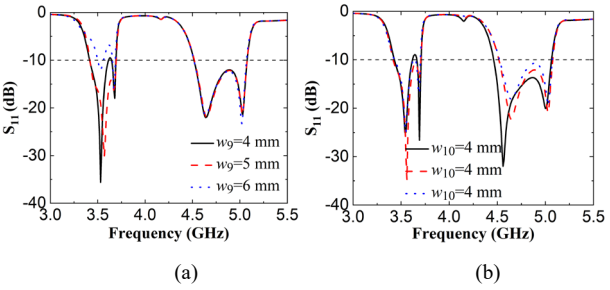

Fig. 7. Reflection coefficient of the proposed antenna with different location of the shorted via. (a) S_{11} with different w_9, and (b) S_{11} with different w_{10}.

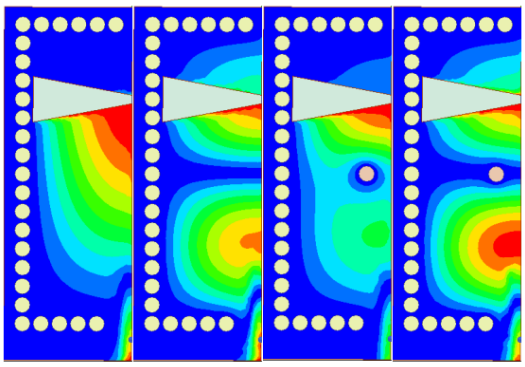

Fig. 8. Electric field distributions of Antenna I with and without shorted via. (a) TE_{110} at 2.2 GHz, without shorted via, (b) TE_{120} at 3.7 GHz, without shorted via, (c) TE_{110} at 3.45 GHz, with shorted via, and (d) TE_{120} at 3.7 GHz, with shorted via.

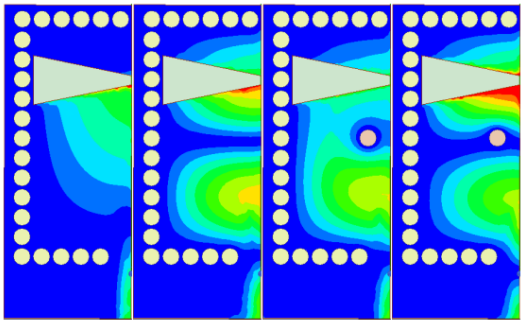

Fig. 9. Electric field distributions of Antenna II with and without shorted via. (a) TE_{110} at 2.45 GHz, with shorted via, (b) TE_{120} at 4.7 GHz, with shorted via, (c) TE_{110} at 4.44 GHz, without shorted via, and (d) TE_{120} at 4.74 GHz, without shorted via.

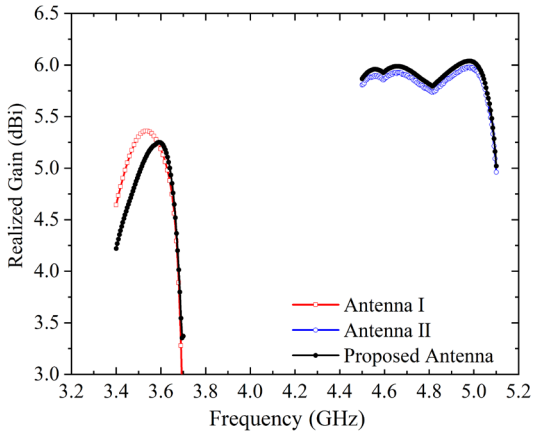

Fig. 10. Simulated realized gains of Antenna I, Antenna II, and the proposed antenna.

3. Measurement Results

To verify the performance, the proposed antenna is fabricated and measured. The reflection coefficients of the fabricated antenna were measured by Agilent E8363 Vector Network Analyzer and the realized gain and radiation patterns were measured with SATIMO SG32 Antenna Measurement System at microwave anechoic chamber.

Figure 11 shows the photo of the fabricated antenna. The simulated and measured reflection coefficient is shown in Fig. 12. At low frequency band of 3.5 GHz, the –10 dB bandwidth of the antenna is 3.47–3.68 GHz, and at high frequency band of 4.9 GHz, the –10 dB bandwidth is (4.62 to 5.16) GHz. The measured results at 4.9 GHz deviate slightly from the simulated. The errors might be caused by insufficient machining accuracy, and the welding of the SMA interface can also result in errors.

Figure 13 shows the measured and simulated gain of the proposed antenna at 3.5 GHz and 4.9 GHz, where simulated results are realized gain and the measured results are peak gain. At 3.5 GHz, the simulated antenna gain is 4.58 dBi. The measured peak gain is about 3.9 dBi, slightly

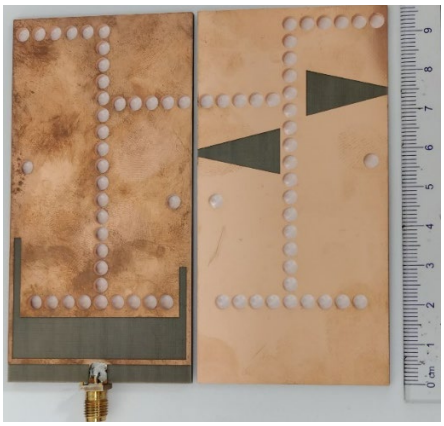

Fig. 11. Fabricated photo of the proposed antenna.

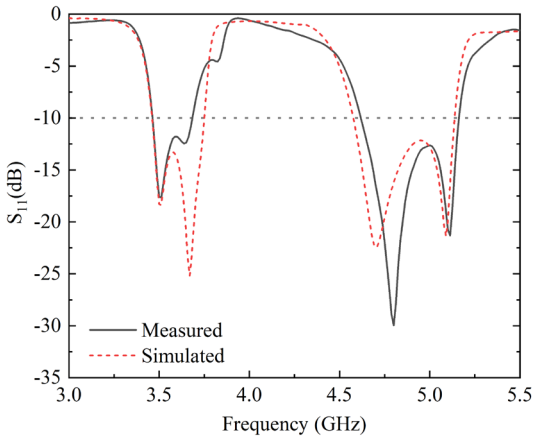

Fig. 12. Simulated and measured reflection coefficient of dual-band antenna.

lower than the simulated. At 4.9 GHz, the simulated gain is 5.8 dBi and the measured is about 5.5 dBi.

Figure 14 shows the measured and simulated normalized radiation patterns of proposed antenna at 3.5 GHz and 4.9 GHz. The measured copolarization results are in accord actual with the simulated. The patterns at 3.5 GHz are omnidirectional, and at 4.9 GHz, the measured patterns have a little distortion. The simulated cross-polarization is also shown in Fig. 14. The simulated cross-polarization level is mostly lower than –10 dB. The linear polarization impurities caused by the irregular slots may contribute to the high cross-polarization levels.

Table 2 shows the performance comparisons between our work and some typically dual-band antenna. It can be seen that the proposed antenna has wider bandwidth with compact size and medium gain.

Ref.	Freq. (GHz)	BW (%)	Gain (dBi)	Size (λ_L^3)
[12]	14/16	2.02/1.46	5.3/4.3	1.12×0.93×0.37
[13]	5.7/9.3	4.5/2.7	8.4/6.35	0.86×0.86×0.048
[14]	8.15/14.2	NM	4/4.8	0.24×0.24×0.174
[15]	2.5/3.4	2/3.8	7.9/8.5	1.06×1.02×0.013
This work	3.5/4.9	6.2/11.0	3.9/5.5	1.09×0.58×0.018

Tab. 2. Comparison of the proposed antenna with referenced designs.

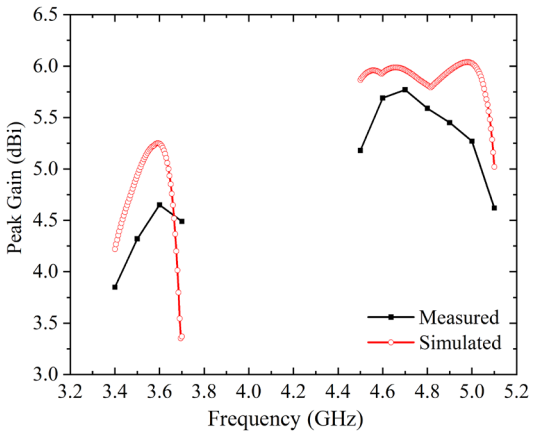

Fig. 13. The measured and simulated peak gain of dual-band antenna.

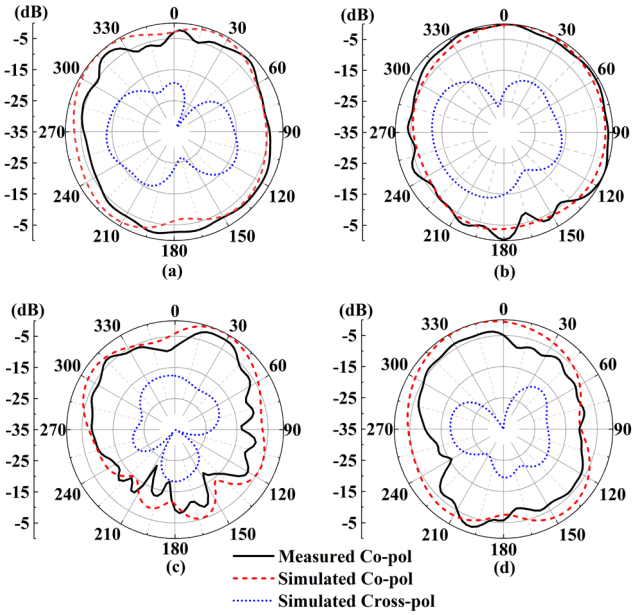

Fig. 14. Simulated and measured normalized radiation patterns of the antenna. (a) E-plane (*y*-*z*) at 3.5 GHz; (b) H-plane (*x*-*z*) at 3.5 GHz; (c) E-plane (*y*-*z*) at 4.9 GHz; (d) H-plane (*x*-*z*) at 4.9 GHz.

4. Conclusion

In this paper, a dual-band HMSIW slot antenna operating at 3.5 GHz and 4.9 GHz is proposed. A 50-Ω microstrip line to 100-Ω coplanar waveguide is adopted to feed the antenna. At 3.5 GHz, the –10 dB bandwidth is 3.47–3.68 GHz, and the gain is 3.9 dBi, as well as the radiation efficiency is 74.2%. At 4.9 GHz, the –10 dB bandwidth is 4.62–5.16 GHz, and the gain is 5.5 dBi, as well as the radiation efficiency is 78.6%. Compared with the traditional SIW dual-band antenna, the bandwidth of the proposed antenna has been greatly improved with maintaining compact size. The proposed antenna has excellent performance in the two frequency bands of n78 and n79, which is suitable for 5G communication systems.

Acknowledgments

This work was supported by the National Natural Science Foundation of China (NSFC) under Grant No. 61871071. (Corresponding author: Xiaolin Yang.)

References

[1] GONG, K., HONG, W., ZHANG, Y., et al. Substrate integrated waveguide quasi-elliptic filters with controllable electric and magnetic mixed coupling. *IEEE Transactions on Microwave Theory and Techniques*, 2012, vol. 60, no. 10, p. 3071–3078. DOI: 10.1109/TMTT.2012.2209437

[2] CHEN, K., LEE, J., CHAPPELL, W. J., et al. Co-design of highly efficient power amplifier and high-Q output bandpass filter. *IEEE Transactions on Microwave Theory and Techniques*, 2013, vol. 61, no. 11, p. 3940–3950. DOI: 10.1109/TMTT.2013.2284485

[3] BELENGUER, A., ESTEBAN, H., BORIA, V. E. Novel empty substrate integrated waveguide for high-performance microwave integrated circuits. *IEEE Transactions on Microwave Theory and Techniques*, 2014, vol. 62, no. 4, p. 832–839. DOI: 10.1109/TMTT.2014.2309637

[4] GAO, Y., ZHANG, F., LV, X., et al. Substrate integrated waveguide filter–amplifier design using active coupling matrix technique. *IEEE Transactions on Microwave Theory and Techniques*, 2020, vol. 68, no. 5, p. 1706–1716. DOI: 10.1109/TMTT.2020.2972390

[5] SONG, K., FAN, Y., ZHANG, Y. Eight-way substrate integrated waveguide power divider with low insertion loss. *IEEE Transactions on Microwave Theory and Techniques*, 2008, vol. 56, no. 6, p. 1473–1477. DOI: 10.1109/TMTT.2008.923897

[6] KHAN, A. A., MANDAL, M. K. Miniaturized substrate integrated waveguide (SIW) power dividers. *IEEE Microwave and Wireless Components Letters*, 2016, vol. 26, no. 11, p. 888–890. DOI: 10.1109/LMWC.2016.2615005

[7] CHEN, H., CHE, W., WANG, X., et al. Size-reduced planar and nonplanar SIW Gysel power divider based on low temperature co-fired ceramic technology. *IEEE Microwave and Wireless Components Letters*, 2017, vol. 27, no. 12, p. 1065–1067. DOI: 10.1109/LMWC.2017.2765558

[8] MUKHERJEE, S., BISWAS, A., SRIVASTAVA, K. V. Broadband substrate integrated waveguide cavity-backed bow-tie slot antenna. *IEEE Antennas and Wireless Propagation Letters*, 2014, vol. 13, p. 1152–1155. DOI: 10.1109/LAWP.2014.2330743

[9] YUN, S., KIM, D. Y., NAM, S. Bandwidth enhancement of cavity-backed slot antenna using a via-hole above the slot. *IEEE Antennas and Wireless Propagation Letters*, 2012, vol. 11, p. 1092–1095. DOI: 10.1109/LAWP.2012.2215911

[10] ASTUTI, D. W., ASVIAL, M., ZULKIFLI, F. Y., et al. Bandwidth enhancement on half-mode substrate integrated waveguide antenna using cavity-backed triangular slot. *International Journal of Antennas and Propagation*, 2020, vol. 2020, p. 1–9. DOI: 10.1155/2020/1212894

[11] SHI, Y., LIU, J., LONG, Y. Wideband triple- and quad-resonance substrate integrated waveguide cavity-backed slot antennas with shorting vias. *IEEE Transactions on Antennas and Propagation*, 2017, vol. 65, no. 11, p. 5768–5775. DOI: 10.1109/TAP.2017.2755118

[12] DECKMYN, T., AGNEESSENS, S., RENIERS, A. F., et al. A novel 60 GHz wideband coupled half-mode/quarter-mode substrate integrated waveguide antenna. *IEEE Transactions on Antennas and Propagation*, 2017, vol. 65, no. 12, p. 6915–6926. DOI: 10.1109/TAP.2017.2760360

[13] GENG, Y., WANG, J., LI, Y., et al. A Ka-band leaky-wave antenna array with stable gains based on HMSIW structure. *IEEE Antennas and Wireless Propagation Letters*, 2022, vol. 21, no. 8, p. 1597 to 1601. DOI: 10.1109/LAWP.2022.3174957

[14] PRADHAN, N. C., SUBRAMANIAN, K. S., BARIK, R. K., et al. Shielded HMSIW-based self-triplexing antenna with high isolation for WiFi/WLAN/ISM band. *IEEE Transactions on Circuits and Systems II: Express Briefs*, 2023, vol. 70, no. 6, p. 1941–1945. DOI: 10.1109/TCSII.2022.3231829

[15] MUKHERJEE, S., BISWAS, A., SRIVASTAVA, K. V. Substrate integrated waveguide cavity-backed dumbbell-shaped slot antenna for dual-frequency applications. *IEEE Antennas and Wireless Propagation Letters*, 2015, vol. 14, p. 1314–1317. DOI: 10.1109/LAWP.2014.2384018

[16] JI, S., DONG, Y., WEN, S., et al. C/X dual-band circularly polarized shared-aperture antenna. *IEEE Antennas and Wireless Propagation Letters*, 2021, vol. 20, no. 12, p. 2334–2338. DOI: 10.1109/LAWP.2021.3110529

[17] LIU, C. M., XIAO, S. Q., WU, K. Miniaturized cylindrical open-ended SIW cavity antenna and its dual-band applications. *IEEE Transactions on Antennas and Propagation*, 2021, vol. 69, no. 8, p. 4390–4400. DOI: 10.1109/TAP.2020.3048553

[18] LI, L., WU, S., PANG, D., et al. A fifth-order single-layer dual-band half-mode SIW filtering antenna with a multifunctional single slot. *IEEE Antennas and Wireless Propagation Letters*, 2021, vol. 20, no. 9, p. 1676–1680. DOI: 10.1109/LAWP.2021.3093062

[19] XU, F., WU, K. Guided-wave and leakage characteristics of substrate integrated waveguide. *IEEE Transactions on Microwave Theory and Techniques*, 2005, vol. 53, no. 1, p. 66–73. DOI: 10.1109/TMTT.2004.839303

[20] HONG, W., LIU, B., WANG, Y., et al. Half mode substrate integrated waveguide: a new guided wave structure for microwave and millimeter wave application. In *2006 Joint 31st International Conference on Infrared Millimeter Waves and 14th International Conference on Terahertz Electronics*. Shanghai (China), 2006, p. 219–219. DOI: 10.1109/ICIMW.2006.368427